24 th EUROPEAN ROTORCRAFT FORUM
Marseilles, France - 15th-17th September 1998

Wind Tunnel Evaluation of a Full Scale Piezoelectric Flap Control Unit*

Référence : TE02

D. Schimke
Eurocopter Deutschland GmbH
München, Germany

P. Jänker
Daimler Benz AG
München, Germany

V. Wendt, B. Junker
Deutsches Zentrum für Luft- und Raumfahrt e.V.
Göttingen/Braunschweig, Germany

Abstract

A collaborative programme is underway to explore the potential of the individual blade control (IBC) technology with regard to two aspects: Control laws are developed and evaluated in flight using an existing blade root control system. In a parallel activity, a smart actuation concept with trailing edge flaps is developed and investigated in a wind tunnel test. This paper focuses on the development, bench testing and wind tunnel evaluation of the trailing edge flaps driven by a piezoelectric flap control unit.

The activities within the development process comprise the aerodynamic layout and the design of the flap control unit on the basis of a piezoelectric actuation system. An additional aspect deals with the integration of this module into a full scale blade segment including the sensor equipment and the interface to the wind tunnel environment. Bench tests were performed in order to verify the designed potential of the actuator itself and the whole flap control unit. For these tests the external loads were derived from aerodynamic calculations and simulated by springs. After final system tests including electromagnetic compatibility (EMC) and temperature tests, the integrated blade segment (wind tunnel model) was integrated into the transonic wind tunnel Göttingen (TWG).

The wind tunnel evaluation itself was performed with several configurations. For the first tests, the model was installed in a fixed configuration and different steady flap deflections and the oscillating flap was measured. These reference tests form the baseline for the more demanding configurations: The influence of the unsteady aerodynamic were investigated by moving the model in an oscillating mode (Forced 1/rev oscillation). In a second evaluation phase, the transfer characteristics of the direct lift and servo effect was investigated by a torsional degree of freedom, which is integrated in the wind tunnel suspension. Because of the different configurations and the additional risk due to the advanced actuation system, the variation of the typical aerodynamic parameters were limited to 3 Mach numbers and focused on a range of the angle of attack which represents the typical aerodynamic conditions of a rotor blade between 80 and 90% radius station in cruise flight condition. However, the various configurations provide a range of results, which refer to several objectives: Reliability and effectivity of the actuation system, comparison of dynamic and static measurements together with a validation of the aerodynamic code and the transfer characteristics of the flap control concept.

The paper gives a short overview about the programme, describes the general design objectives, the development process of the flap control unit, the wind tunnel facility together with the different configurations and presents results from the test campaign itself.

* Presented at the 24th European Rotorcraft Forum in Marseille, Germany, September 15-17, 1998

1. Description of the Programme

The rotor active control technology (RACT) programme, equally shared by the German Ministry of Research and Technology (BMBF) and by resources of the partners, forms the baseline of the activities described in this paper. The partners within the RACT-programme are EUROCOPTER DEUTSCHLAND GmbH (ECD, Project leader), the Deutsches Zentrum für Luft- und Raumfahrt e.V. (DLR), the Daimler-Benz research establishment (DB), the Technical University of Braunschweig and ZF Luftfahrttechnik GmbH (ZFL). The whole programme comprises fight test activities with a blade root control system and wind tunnel tests with a full scale piezoelectric flap control unit. A description of both parts of the RACT programme is given in Ref 1. This paper focuses on that part of the programme, which deals with the development of a piezoelectric flap control unit integrated in a wind tunnel model and the evaluation in the Transsonic Wind Tunnel Göttingen (TWG).

2. Layout of the Flap Control Unit

For the general layout of the flap control unit the relationship between the torsional stiffness of the blade design and the type of the control law respectively the azimuth region which has to be mainly influenced lead to different optimum flap designs. The data base for the present design assumes a torsional eigen frequency of 4-5/rev and the investigated control laws are a time domain vibration controller and a control law for the reduction of the external noise during approach flight. For this assumption a relative chord of the flap of 15 % for a high servo effect at low hinge moments was selected (Ref 1).
Additional design criteria for this chord were manufacturing aspects and the achievable force deflection characteristic of the flap control unit.

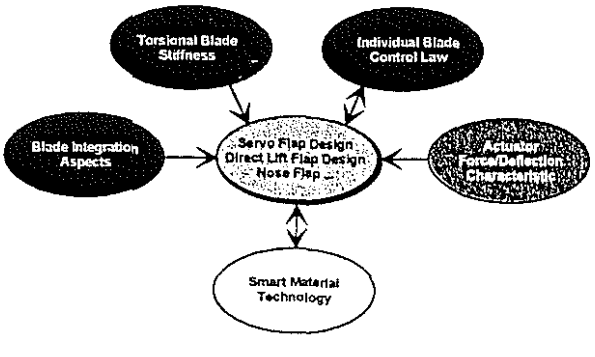

Figure 1: Main aspects for the general layout of several flap designs.

Figure 1 shows the main aspects for the general layout of several flap designs.

2.1. Objectives and Requirements

As mentioned above, the reduction of the cabin vibration and the external noise were the two main objectives for the general layout of the flap. The reason for these main objectives were, that for both areas promising results from wind tunnel and flight tests exist (e.g. Ref 2) and that both control strategies are investigated in flight using a blade root IBC-system in a parallel activity of this programme. Recent results of this activity are presented in Ref 3.

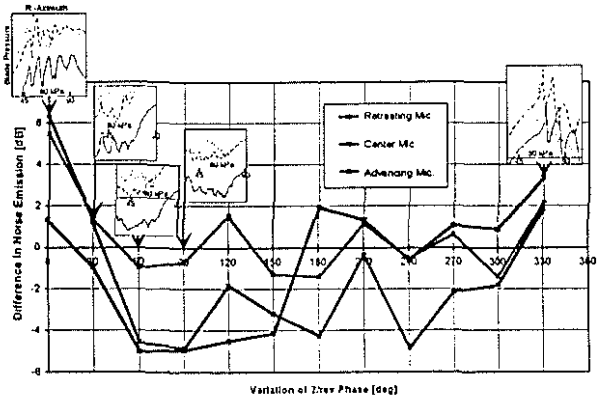

Figure 2: Reduction of blade vortex interaction noise by a 1 degree 2/rev blade root control input

A short summary of quite promising, very recent results from the first open loop flight tests within the evaluation phase, which are discussed in more detail in Ref 4, is shown in Figure 2:

- The blade pressure vs rotor azimuth shows clearly the blade vortex interaction (BVI) for the baseline helicopter and non optimum 2/rev phases.
- For a phase of 60 and 90 degree this BVI condition could be completely suppressed and the noise on ground (plotted is the noise measured by the 3 microphones located at the certification positions) was noticeable reduced.
- In addition, the cockpit vibrations were reduced by 50 to 80% in the three axes for the minimum noise condition.

The second control strategy, which will be tested in flight in the second evaluation phase is the reduction of the cabin vibration. For this objective a complete closed loop design was developed for a time domain vibration controller (Ref 1, Ref 5). The used computer code for the controller design is CAMRAD II (Ref 6), validated with flight test

data. The simulation results in Figure 3 show one out of several concepts of the vibration controller (Design objective: Suppression of 3 hub loads, e.g. pitch/roll moment and vertical force): Switching the blade root actuation system on (upper plot), the hub loads are reduced nearly to zero within three rotor revolutions.

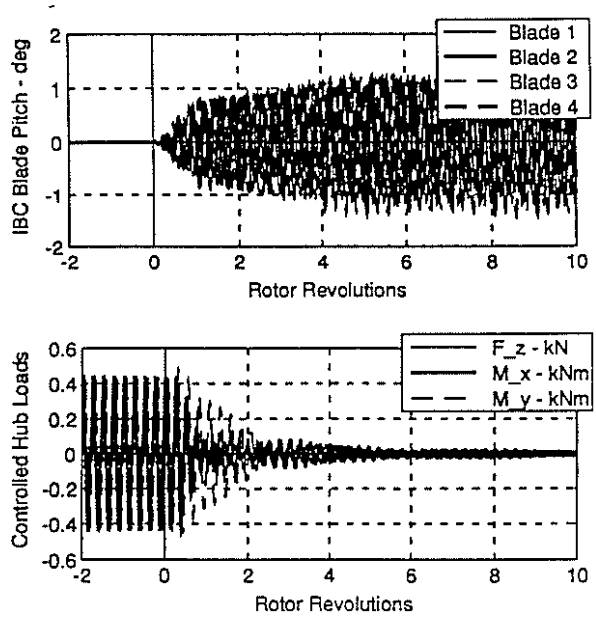

Figure 3: Suppression of 4/rev hub loads in forward flight

The parallel activities with the blade root control concept, tested in flight, demonstrate the potential of IBC, which has to be required also from the flap control system. In addition, this test campaign is helpful for the validation of the comprehensive rotor models and the control law design methodology needed for the layout of the individual control strategies.

As a reasonable first step for special calculations with regard to the design parameters of the flap, the CAMRAD II code used for the blade root control law design was extended by a flap control module. The aerodynamic coefficients for this module were taken from the Navier-Stokes calculations described in Chapter 2.2.

Figure 4 shows the same closed loop simulation shown in Figure 3 but using the flap control module. This calculation shows, that a certain correlation between the blade root and the flap control strategy can be derived and that for the assumed aerodynamic layout one degree blade root control input corresponds to a 5 degree flap amplitude. A more detailed analysis of the lift distribution gave additional informations in terms of a more generalised requirement for the control power of the flap.

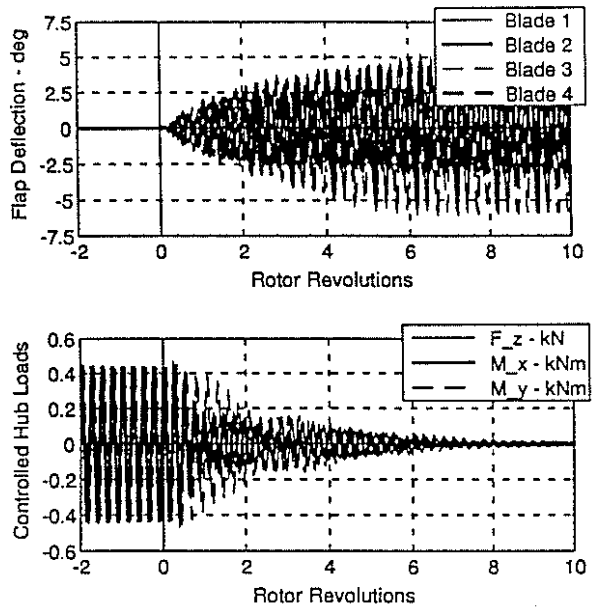

Figure 4: Requirement for the flap control power, derived from the vibration control law and correlation with the blade root control strategy

2.2. Aerodynamic Layout

The aerodynamic layout of the flap was performed by two steps: The preliminary layout of the hinge moment was estimated by 2-D quasi-steady calculations varying the geometry for different flap deflections and flap chords. The aerodynamic model included compressibility and boundary layer effects (Ref. 7, Ref. 8). These calculations were also the starting point for the general layout of the actuation system.

Selected cases out of the preliminary design points were calculated with a more complex aerodynamic code including friction, unsteady aerodynamics and the oscillating flap motion (Ref. 9, 10, 11, 12). The results were used for the final specification of the required actuator performance, for the calculations with CAMRAD II (See Chapter 2.1) and for the preparation of the wind tunnel tests.

The assumed aerodynamic condition refers to a typical cruise flight condition of a light helicopter like EC135. The selected Mach numbers and angle of attack range of refer to the fore/aft, advancing and retreating azimuth angle of the 85% radius station of the rotor blade. The geometrical data of the assumed rotor blade are as follows:

Radius: 5.1 m
Chord: 0.3 m
Flap length/Position: 0.5 m/0.8-0.9 R
Relative flap chord: 15% (Final config.)

Figure 5 shows the hinge moments from the two aerodynamic codes used for the preliminary and final design in comparison with the available hinge moment of the actuators measured during the bench tests (Compare Chapter 3).

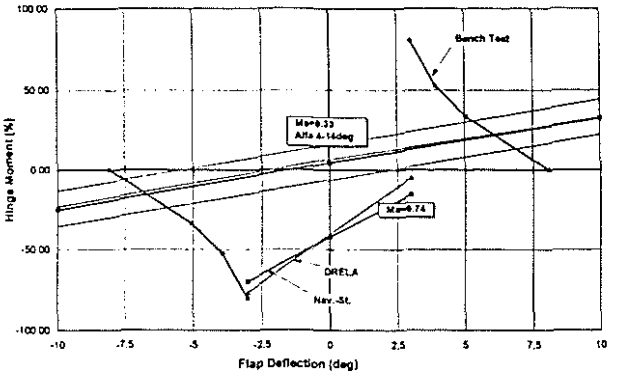

Figure 5: Aerodynamic hinge moments calculated by two methods and available hinge moments from the actuator derived from bench tests

The wind tunnel test showed, that this quasi-steady estimation was a bit too conservative. In comparison to the achieved values during the wind tunnel tests (See Table 2), more actuator performance was reached than estimated from Figure 5.

3. Development of the Integrated Flap Control Unit and Wind Tunnel Model

3.1 General Design Aspects for the Actuator

A major design aspect is to integrate the flap actuator mechanism completely inside the blade geometry requiring a compact design of the unit. Extreme requirements are placed on the flap drive which cannot be met by conventional technologies: A high mechanical load due to the high centrifugal acceleration of 1000 g, small installation volume, high dynamics and stroke resolution with a high mechanical actuator performance. Only the piezoelectric actuator system one of the most suitable drive principle from today's point of view.

Piezo actuators represent a new technology that offers a host of advantages. In combination with signal processing electronics, the good mechanical and electrical integrability of piezoelectric actuators make these devices key elements in innovative intelligent systems. Despite of these advantages, piezoelectric actuators have so far only found use in niche applications. Today, there are just a few model designs of mechanically efficient piezoelectric systems, the operating behavior of piezoelectric actuators has yet to be adequately characterized.

Actuators based on mechanically active materials (smart materials) exploit physical solid-state effects and transform electrical control energy directly into mechanical work. Piezoelectric materials are particularly promising. The outstanding properties of piezoceramics are:

- Controllability and resolution
- Speed
- Energy density (Ref 13)
- Mechanical integrability, as based on solid-state technology.

Due to the geometry of the blade only a short lever can be installed inside the profile to actuate the pivoted flap. The required actuator stroke in the mm range with actuator forces in the range of 2000 N is about one order of magnitude higher than the stroke capacity of previously available piezoelectric actuators. Figure 6 shows the force stroke characteristics of conventional piezoelectric actuators. Benders provide too low force and stack actuators have too small stroke capability. Due to the low elongation capacity of piezoelectrical materials, stack actuators are unsuitable. A design for a technical amplification mechanism is the hybrid actuator developed by Daimler-Benz Research in recent years.

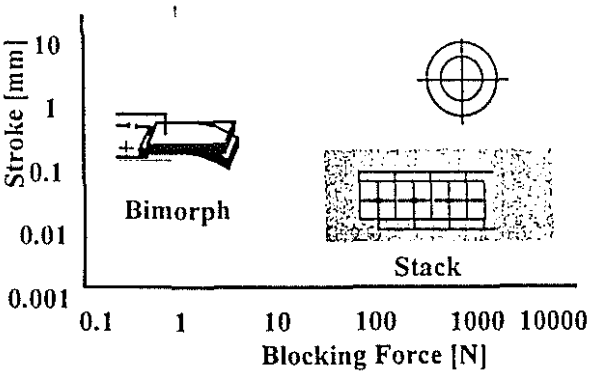

Figure 6: Working Range of Piezo Actuators

A hybrid design method, comprising a piezostack with a hydraulic or mechanical step-up gear, is suitable for actuator forces F_b > 500 N. The step-up gear must meet the following requirements:

- Stiff support of the piezostack
- No mechanical play

- No/slight friction
- High energy efficiency: low elastic energy losses
- Gear ratio of 1:10
- Low weight relative to the piezostack
- Production oriented design

In order to implement a step-up gear, a variety of differing designs was put forward. Some of these designs were discussed by Prechtl (Ref 14). With the aim of indicating the limitations of the hybrid construction method, the influence of the mounting frame alone on the overall performance of the hybrid actuator will be discussed in the following. An important objective in optimising the design is to maximise the specific energy density. The maximum specific energy density was assessed and optimised.

The reduction of the blocking force due to the ratio of the stiffness of piezostack to frame and the reduction of the free stroke caused by elastic retroactive forces (friction, elastic forces) results in a energy efficiency factor smaller than 1:

$$\eta_{energy} = W_{hybrid}/W_{piezo}$$

To boost the energy efficiency the stiffness of the frame must be increased. But a heavy construction is not allowed because of the high centrifugal acceleration. An important Figure of merit is therefore the mass efficiency factor:

$$\eta_{mass} = \eta_{energy}\, m_{hybrid}/m_{piezo}$$

3.2 Design of the Hybrid Actuator

An integrated design is considered to be the optimum construction method for a weight and volume optimised hybrid actuator. The stiff mounting frame, which is required in any case, is designed through the integration of joints as a gear. In order to ensure freedom from play and wear, flexures are used as joints. Figure 7 shows the diamond-shaped geometry of the gear. The new actuator design called the DWARF Actuator is highly energy efficient. Due to the geometric arrangement, an expansion movement of the piezostack is transformed into a pulling movement. Critical elements of the design are the flexures that are loaded in axial and bending directions. The flexures act on the one hand as a spring load on the piezostack and reduce the free stroke. On the other hand, the flexures are a determining factor for the stiffness of the frame. A compromise must be made between high axial stiffness and low bending stiffness. The effectivity of the gear was optimised decisively by being designed as a multiple frame. With high axial frame stiffness, the bending stiffness of the joints is reduced, the material load on the joints is decreased and the stroke increased. The detailed computational optimisation of the DWARF system was effected using analytical methods and FEM. The dynamics of the hybrid actuator is very good, the first resonance frequency of the flap actuator system lies at 220 Hz.

Integrated lightweight and compact design:
- the stiff mounting frame is designed through the integration of joints as the gear
- flexures to avoid wear and play

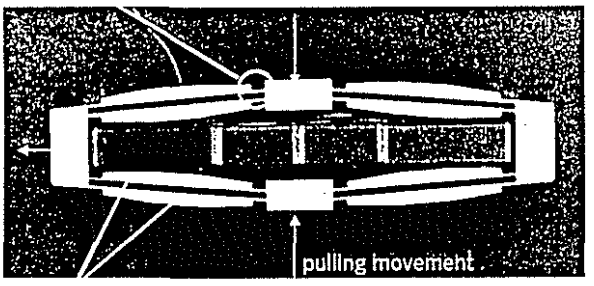

multiple frame design
- reduced material load
- high axial stiffness
- low bending compliance

Figure 7: Hybrid actuator DWARF

Table 1: Technical Data of DWARF

Blocking Force	720 N
Free Stroke	1.1 mm
Energy Efficiency	83 %
Resonance Frequency	220Hz
Mass	400 g
Mass Efficiency	33%

3.3 Design and Test of the Integrated Flap Control Unit

The actuators are near the nose of the airfoil in order to maintain the centre of gravity at 25% chord. The actuators are acting parallel via pull rods and a hinge lever on the pivoted flap. A stiff construction is necessary to achieve a highly efficient energy transport. The joints and the pull rods are constructed to be mechanically stiffer than the hybrid actuator. The lightweight flap causes a small inertia. Thus the first mode of the actuator flap unit is at a very high frequency (Approximately 180 Hz). The endurance and performance of the actuator flap unit was tested

prior to the wind tunnel test in a bench set-up. Attention was focused on the dynamic properties of the system. During the tests the aerodynamic load was simulated by a spring. The result of this test is included in Figure 5. Figure 8 shows the flap control unit integrated in the wind tunnel model.

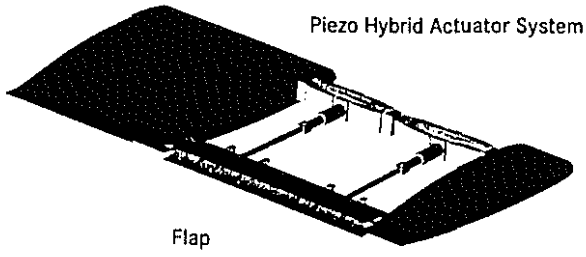

Figure 8: Piezoelectric Flap Control Unit

3.4 Design of the Wind Tunnel Model

Figure 9 gives an overview about the total wind tunnel model with the wind tunnel adapter and the view inside to the integrated actuators, the stiffening ribs between the flap control rods and the flaps itself.

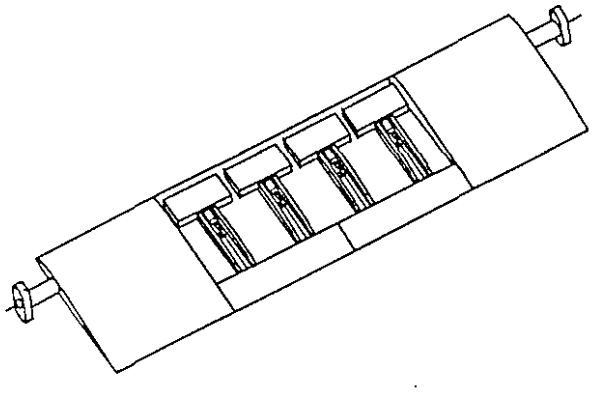

Figure 9: Wind Tunnel Model with Integrated Piezoelectric Flap Control Unit

The shell of the wing model is made out of carbon fibre and in principle in a well known and conservative design method. Fabric carbon fibre with diagonal fibre orientation were used to take up the torsion loads in the outer part of the wing shell. To take up the bending loads inside the wing section unidirectional carbon fibre layers were applied in the area of the 25% line. At the ends of the wing two aluminium adapters are the fixation points for the wind tunnel facility.

For the integration of the piezo actuators, the control rods and the flaps itself it was ingenious to install all these elements on one base plate. The advantage of this concentration was, that all the adaptation and adjustment work for the flap control unit could be done in parallel to the development of the wind tunnel model wing. With the width of the two flaps a part on the lower side of the wing section beginning at 7 % chord was used for the base plate to place in the actuators, the control rods and the flaps.

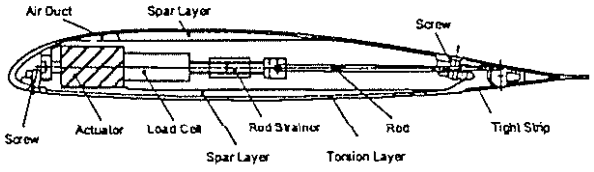

Figure 10: Sectional View of the Blade Segment

Figure 10 gives an overview about a section in the middle part of the blade segment. The torsional stiffness and the airfoil contour stability is guaranteed by screws around the border of this removable wing section part. The stability and the stiffness in the bending mode is given by three metallic bolts in the 25 % line area on each side of the base plate. These bolts are passed on the spar loads from the outer upper part of the right wing side to the removable part and further to the other outer upper part of the wind tunnel model on the left hand side. The removable part of the model has the same fibre layer design in the torsion shell and in the spar like the main part of the wing. To guarantee the stiffness of the base plate in chord direction, it was necessary to install several stiffening ribs between the position of the actuators and the fixing points of the flap bearings.

To provide a cooling of the actuators, a channel with holes was installed above the actuators for blowing air on the piezo elements. Alternative, to protect the model against fire induced by electrical faults it was possible to blow nitrogen via the same channel into the model. However, during the wind tunnel trials no cooling or other described provisions were needed.

Due to the integrated actuation system in the wind tunnel model and the unsteady aerodynamic measurement, a comprehensive sensor equipment was integrated in the wind tunnel model. For the control and monitoring of the actuation system the linear displacement of the actuator force, the flap deflection and the temperature of the actuators was measured. For a supplementary aerodynamic measurement in addition to the piezoelectric balance, integrated in the wind tunnel suspension, the pressure distribution was measured by 49 differential

pressure sensors (Kulites). Figure 11 shows the distribution of these sensors. Inside the model the reference signals of all sensors were combined.

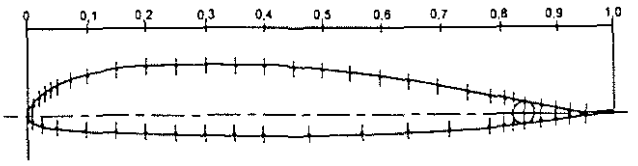

Figure 11: Distribution of Pressure Sensors integrated in the Wind Tunnel Model

4. Wind Tunnel Evaluation

4.1 Transsonic Wind Tunnel Göttingen (TWG)

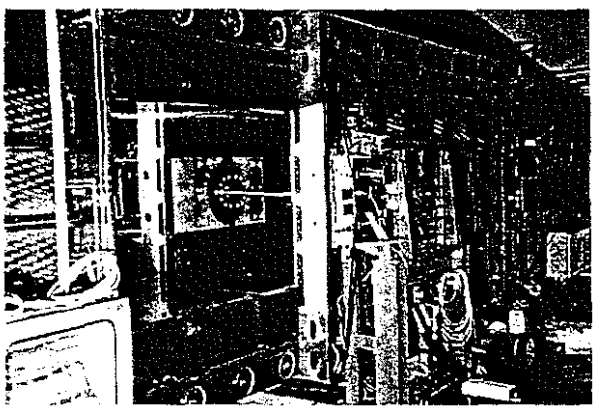

Figure 12: View of the whole test section

The wind tunnel tests were conducted in the transonic wind tunnel of DLR in Göttingen. The recently modified wind tunnel is a continuous, single return facility with three exchangeable square test-sections (size: 1 x 1 m^2) for the subsonic, transonic and supersonic speed regime. The absolute size of the test section is ideally suited for 2-D wing experiments because on the one hand it is large enough to permit the use of models equipped with sophisticated measurement techniques (pressure transducers etc.), on the other hand it is small enough to keep the effort concerning the structural dynamic properties of the test set-up and adjustments of the mounting system in reasonable limits. The same is valid for the application of advanced optical measuring techniques such as pressure sensitive paints (PSP) or particle image velocimetry (PIV). The measurements were performed in the transonic test section with perforated walls. Alternatively a test section with adaptive walls is available. Especially for the measurements within the RACT programme the Mach number range was extended down to Ma = 0.3. A view of the whole test section is presented in Figure 12.

The 2-dimensional wing model with a chord length of 0.3 m, a span of 1 m and an OA312 airfoil is attached on both ends to a cross spring and a both sided torsional excitation, providing a fully symmetrical set-up. Between the outer torsional exciters and the inner cross spring a piezoelectric balance is mounted in order to measure steady and unsteady forces. On each side the balance consists of four multi-component force transducers. The main feature of such wind tunnel balances is their high stiffness. Thus piezoelectric balances are in particular suitable for dynamic measurements (Ref 15, 16). In addition the pressure distribution is measured for one cross section, especially for the analysis and the validation of the dynamic measurements. Four laser triangulators determine the pitching angle $\alpha(t)$ of the wing itself. This angle is different from the adjusted angle at the torsional exciters, if the torsional spring is installed. Figure 13 shows the test set up for the different suspensions providing the configurations used during the evaluation tests.

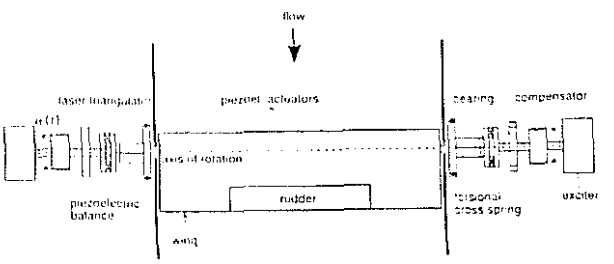

Figure 13: Schematic sketch of the test set-up suited for fixed configuration, forced pitch oscillations and torsional degree of freedom.

4.2. Execution of Tests

The whole test campaign was performed from the 4th to the 20 th of May in 1998. Table 2 gives an overview about the tested configurations, the aerodynamic conditions and the achieved flap deflections.

The piezoelectric flap control unit worked without any failure throughout the test campaign and the performance of the flap control unit was better than estimated by the bench tests (Figure 5).

Table 2: Overview about the tested configurations

Suspension of Model	Flap Motion	Ma	Max. Angle of Attack	Max Flap Deflection
Fixed	Fixed	0.3	Ref. Polar	0.0
Fixed	Fixed	0.54	Ref. Polar	0.0
Fixed	Fixed	0.74	Ref. Polar	0.0
Fixed	Fixed, 1 to 5/rev	0.33	+4.1→+14.1	+7.0→-8.0
Fixed	Fixed, 1 to 5/rev	0.54	-1.0→+9.0	+7.0→-7.0
Fixed	Fixed, 1 to 5/rev	0.74	-0.85	+6.0→-4.0
Forced 1/rev	Fixed, 1 to 5/rev	0.33	9.1 ±5.0	±5.0
Forced 1/rev	Fixed	0.33	-> Dyn. Stall	+5.0
Forced 1/rev	Fixed, 1 to 5/rev	0.54	4.0 ±5.0	±5.0
Tors. DOF	Fixed, 1 to 5/rev	0.33	9.1±Variable	±2.5
Tors. DOF	Fixed, 1 to 5/rev	0.54	4.0±Variable	±2.5

An advantage of the removable test section of the TWG, was the flexible change between the possible types of suspension, described above. Therefore, the integration of the torsional DOF could be performed very fast after the completion of the test period with the fixed configuration and and the forced pitch oscillation.

4.3. Results from the Evaluation

Reference Measurements: Before the evaluation tests were started, reference points were measured which were defined according to existing airfoil data from wind tunnel tests performed by ONERA. Applying the wind tunnel correction parameters valid for the TWG, the same lift curve slope was measured as for the ONERA test. However there still remain differences especially for the maximum achievable lift which result mainly from the higher blockage in the TWG. In spite of the larger test section of the TWG, the size of the full scale model led to the higher relative blockage effect.

Static and dynamic measurements: Tests were performed with fixed and oscillating airfoil (7 Hz), in order to compare steady and unsteady aerodynamic mesurements and to validate existing 2-D codes (Ref. 8). In addition both measurements were performed with static flap deflection and oscillating flap (7 to 35 Hz). For the cases with oscillating airfoil and flap the phase between the airfoil and pitch oscillation was varied too. A first analysis of these data in comparison with the comprehensive numerical model is performed in Ref 11. A typical result of these data is shown in Figure 14 for Ma=0.54. The lift and moment coefficient is integrated from the pressure distribution whereas the drag coefficient is taken from the piezoelectric balance, which shows reliable values for the dynamic changes. The lift coefficient shows the superimposed large change of the lift resulting from the forced pitch oscillation (7 Hz) and the direct lift effect due to the 35 Hz oscillation of the flap. The pitching moment coefficient shows quite large changes mainly caused by the flap control, which is very effective about the pitch axis. However, in this configuration no torsional degree of freedom is available and therefore the servo-effect (Lift due to airfoil torsion) is not included. The main purpose for the tests in this configuration was the evaluation of steady and unsteady aerodynamics. These data will be further used for the analysis of aerodynamic phenomena, the generation of a data base and the validation of numerical codes.

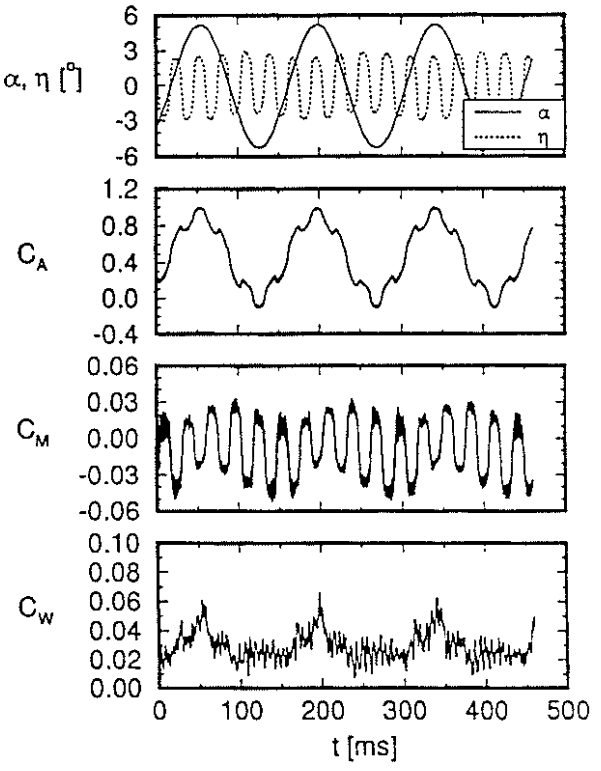

Figure 14: Superimposed Oscillation of the Airfoil (7 Hz,4° ± 5°) and flap (35 Hz and ± 2.5°) at Ma=0.54.

Dynamic Stall: For the Mach number of 0.33 representing the aerodynamic condition of the retreating blade, the dynamic stall characteristic of the airfoil was investigated for a fixed flap deflection of 3° downwards. Figure 15 shows the results of three test series at Ma=0.33 and varying angle of attack up to stall condition. The difference between the steady and unsteady measurements shows the typical dynamic stall effect at the retreating rotor blade of the helicopter, which allows an higher angle of attack than measured in the steady condition. In addition, the direct lift effect due to a flap deflection of 3 deg is shown. Again, the servo effect (Lift decay due to blade torsion) is not included in this configuration, but this effect is

than measured in the steady condition. In addition, the direct lift effect due to a flap deflection of 3 deg is shown. Again, the servo effect (Lift decay due to blade torsion) is not included in this configuration, but this effect is very small at Ma=0.33 and for a steady flap deflection. These tests showed, that the flap deflection was controllable up to extreme stall conditions and the lift can be controlled within the aerodynamic limits defined by the flap size. However, for a more effective control of the retreating blade stall a larger flap or nose flap would be much more effective.

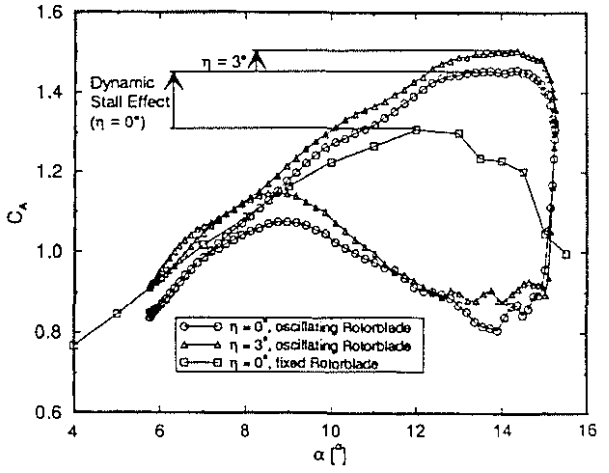

Figure 15: Investigation of Dynamic Stall Characteristic with and without Flap Deflection

Tests with torsional degree of freedom (DOF): For a better understanding of the aerodynamic conditions of a flap controlled rotor, a torsional DOF was integrated in the wind tunnel suspension using a torsional spring. The dynamic layout simulates the first torsional mode of the rotor blade at about 28Hz (4/rev). In this configuration the direct lift vs servo effect was investigated. For the analysis of the total lift in relation to the dynamic and aerodynamic design parameters the distinction between direct lift and lift due to torsional DOF (Servo-effect) is important. Direct lift is the lift, which is generated by the flap deflection without any influence of the torsional DOF. This part of the lift is dominating, if the total lift in Figure 16-19 follows the time history of the flap motion. The servo effect lift is the change of lift due to the elastic twist of the blade. It is dominating, if the total lift follows the oscillation of the angle of attack. However, this simulation of the torsional DOF can only take into account the basic flap control principle of the torsional DOF of a rotor blade. The effect of the full blade area and the complexity of the aerodynamic condition of the rotor blade number like the flap and lag DOF, coupling effects etc. are of course not taken into account for this test condition. Nevertheless, some interesting effects for the Mach number 0.33 can be shown, which are directly influenced by the general layout parameters discussed in Figure 1. For the assumed design parameters the servo effect is dominating at high Mach numbers (Higher dynamic pressure). The influence of the Mach number respectively rotor azimuth region on the two parts of the lift is discussed in more detail in Ref 1.

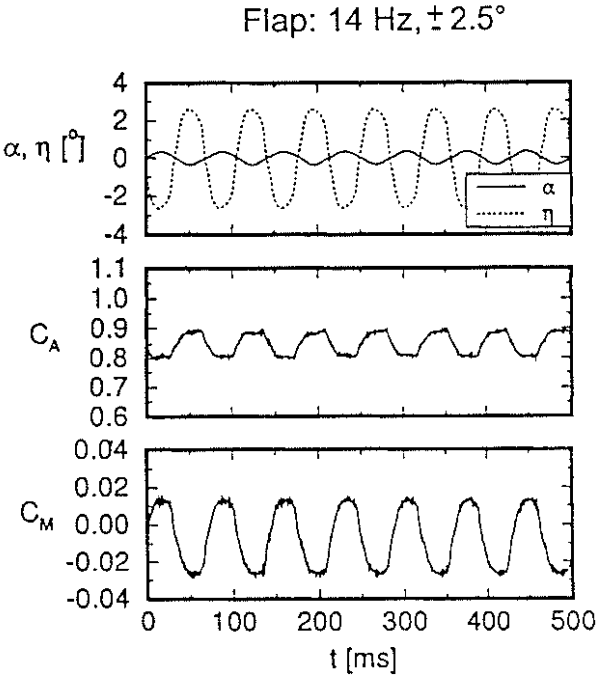

Figure 16: Direct lift effect dominates the total lift at low dynamic pressure (Ma=0.33) and low flap control frequency. Servo effect acts against direct lift effect.

Figure 20 summarises the results of Figure 16 to 19 and shows, that for the quite simple test configuration a quite complex transfer characteristic is obtained at Ma=0.33. For a steady flap deflection and low flap control frequency, the direct lift dominates the total lift (Figure 16). Some loss is induced by the low torsional stiffness of the suspension (Servo effect). This loss is increased with higher flap control frequency and consequently a frequency can be adjusted, where the two effects cancel each other. For the selected design parameters this frequency is slightly above 21 Hz. With a control frequency of 21 Hz (Figure 17) this condition is nearly reached. Maximum transmissibility between flap deflection and lift is reached close to the resonance frequency due to maximum blade torsion.

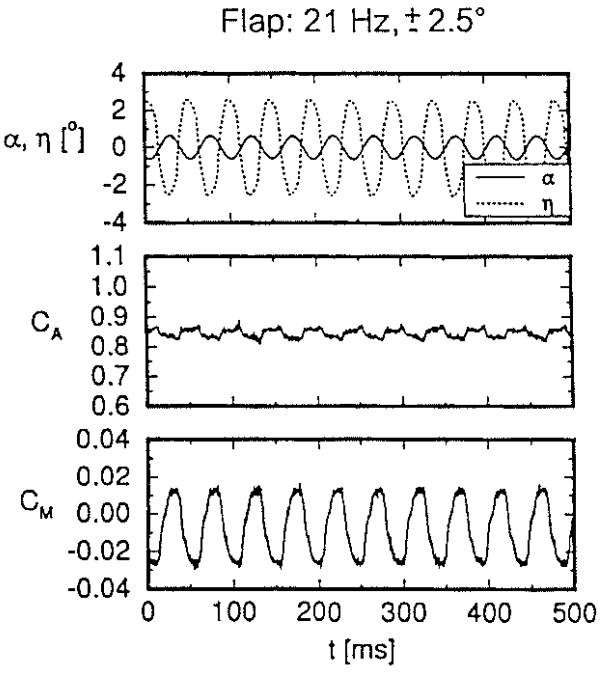

Figure 17: Cancelling of direct lift effect and servo effect at increased flap control frequency

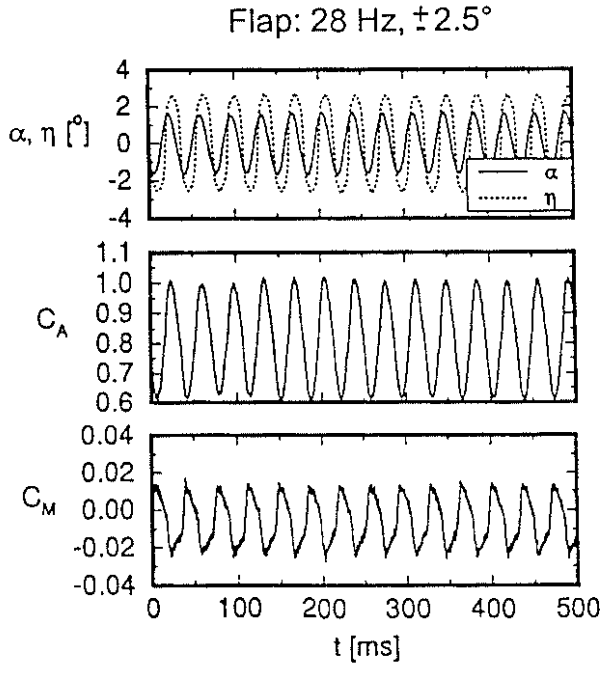

Figure 18: Maximum effeciency around the resonance condition due to servo effect.

The time history of the lift curve shows clearly, that it follows the torsional oscillation (Angle of attack). This indicates, that the servo effect dominates the lift in this condition (Figure 18). Beyond the resonance frequency two effects define the lift due to flap deflection. First, the servo effect is strongly reduced with increasing frequency and second, the phase change of about 180° influences the sense of this effect: Servo effect and direct lift act in the same sense. This phenomenon leads to the quite good transfer characteristic beyond the resonance frequency. However, for a controller design the changed phase of the servo effect has to be taken into account.

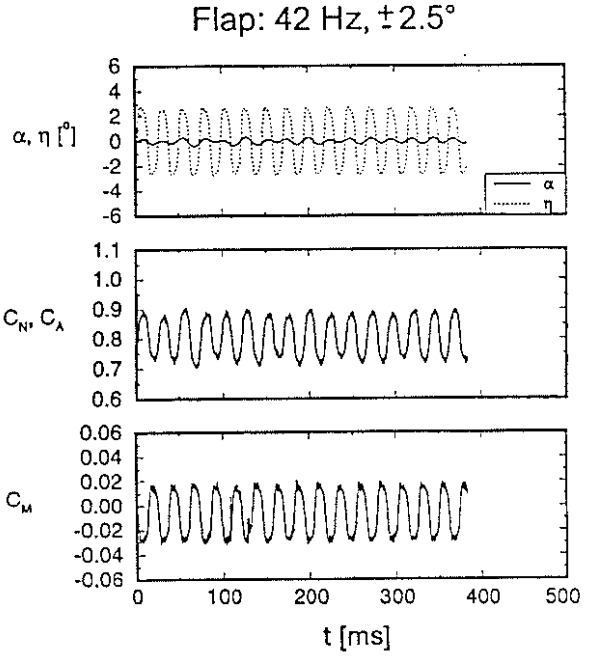

Figure 19: Beyond the resonance condition, the servo effect is strongly reduced with increasing frequency. Due to the phase shift of the servo effect by about 180 deg, the dominating direct lift effect and servo effect act in the same sense.

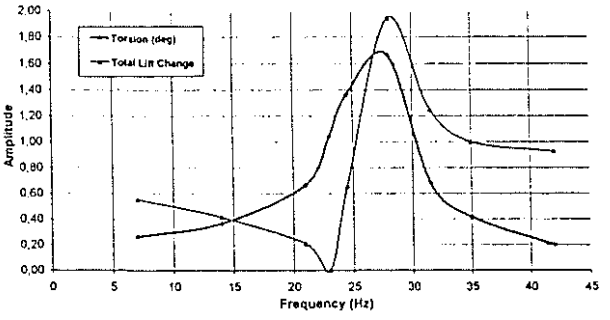

Figure 20: Transfer Characteristic of Total Lift at different Flap Control Frequencies

5. Future Activities

The next step in the development of a flap control unit will be the testing on a centrifugal test bench. For these tests an optimisation process for the design has already been started. End of this year the whole unit will be tested at about 1000g. After these tests, the integration of the flap control unit in full scale rotor blades is planned together with the testing on the whirl tower. This milestone will be the last important step before testing the flap in flight. An important design philosophy of EUROCOPTER for the development and test of the flap control principle was the beginning of the whole development process in a full-scale realisation, because this has a decisive influence on important feasibility aspects. The evaluation of bench and wind tunnel tests presented in this paper are the first step in this process. The results encourage to continue the development.

6. Summary

According to the general design aspects for a flap control principle, one design was selected which takes into account a typical torsional stiffness of a rotor blade, actuator performance and integration aspects and the control laws for the reduction of BVI noise and vibrations. The parallel evaluation of these control laws by a blade root control system in flight within the RACT programme forms also an important baseline for the development of the flap control principle: The improvements achieved by the blade root control system can be taken as a reference for the requirements for the flap control system, the validation of tools similar for the two control principles can be based on flight tests and the methodology for the control law design can be evaluated in parallel to the realisation process of the flap controlled rotor.

The aerodynamic layout especially with regard to the hinge moments was an important optimisation loop for a well designed actuator performance and flap size. Using results from the bench tests together with the calculated aerodynamic forces the achievable flap performance during the wind tunnel tests was well predictable.

The optimised design of the piezo hybrid actuator system is an encouraging design with regard to performance, weight and volume. The rotor blade integration concepts are promising.

According to the different types of suspension systems and configurations tested, the results of the wind tunnel evaluation will be analysed with regard to manifold aspects. Recent results can be summarised as follows:

- The reference tests show consistent results in comparison with the tests from the original airfoil measurements performed by ONERA.
- The steady and unsteady measurements with fixed and oscillating flap give a good data base for the code validation and was a test for the actuator performance in steady and unsteady conditions up to dynamic stall and up to a maximum Mach number of 0.74.
- The tests with a torsional DOF demonstrated the transfer characteristic of the lift due to flap control inputs below, near and above the eigen frequency of the torsional DOF, derived from a typical rotor blade design. The test showed some interesting effects due to the superimposed direct lift and servo effect.

7. References

1. Schimke, D., et al., "Individual Blade Root Control by Servo-Flap and Blade Root Control - A Collaborative Research and Development Programme", 23rd European Rotorcraft Forum, September, 1997, Dresden, Germany

2. Teves, D., et.al., "The Role of Active Control in Future Rotorcraft", 21. European Rotorcraft Forum, Saint-Petersburg Russia, pages 10.1-10.17, August 30 - September 1, 1995.

3. Schimke, D., Arnold, U., Kube, R., „Individual Blade Root Control Demonstration - Evaluation of Recent Flight Tests", American Helicopter Society, 54th Annual Forum, Washington, D.C., May 1998

4. Schöll, E., et al., "Noise Reduction by Blade Root Actuation - Validation and Analysis of Flight and Wind Tunnel Tests", 24th European Rotorcraft Forum, September 1998, Marseille, France

5. Dieterich, O., "Application of a Modern Control Technology for Advanced IBC Systems", 24th European Rotorcraft Forum, September 1998, Marseille, France

6. Johnson, W., "Technology Drivers in the Development of CAMRAD II", American Helicopter Society, San Francisco, California, January, 1994.

7. Drela, M., Giles, M.B., "ISES: A Two-Dimensional Viscous Aerodynamic Design and Analysis Code", AIAA 25th Aerospace Sciences Meeting, AIAA-86-0424, January 12-15, 1987, Reno, USA

8. Sobieczky, H., „Geometry Generation for Transonic Design - Recent Advances in Numerical Methods in Fluids", Vol. 4, Ed.W.G. Habashi, Swansea; Pineridge Press, pp.163-182 (1985)

9. Geissler, W., „Instationäres Navier-Stokes Verfahren für beschleunigt bewegte Profile mit Ablösung", DLR-FB 92-03(1992)

10. Geissler, W., Sobieczky, H., „Dynamic Stall Control by Variable Airfoil Camber", AGARD 75th Fluid Dynamic Panel Meeting and Symposium on Aerodynamics and Aeroacustics of Rotorcraft. Oct. 10-14, 1994, Berlin, Germany

11. Geissler, W., Chandrsekhara, M. S., Platzer, M. F., Carr, L. W., „The Effect of Transition Modeling on the Prediction of Compressible Deep Dynamic Stall", 7th Asian Congress of Fluid Mechanics, Dec. 8-12, 1997, Madras, India

12. Geissler, W., Sobieczky, H., Volmers, H., „Numerical Study of the Unsteady Flow on Pitching Airfoil with Oscillating Flap", 24th European Rotorcraft Forum, September 1998, Marseille, France

13. Jänker,P., Martin, W., „Performance and Characteristics of Actuator Materials", Fourth International Conference on Adaptive Structures, 2-4. November 1993, Cologne, Germany

14. Prechtl, E. F., Hall, S. R.,"Design of a High Efficiency Servo-Flap Actuator for Helicopter Rotor Control", Smart Structures and Materials, San Diego, 1997

15. Schewe, G., "Force Measurements in Aero-elasticity Using Piezoelectric Multicomponent Transducers", Int. Forum on Aeroelasticity and Structural Dynamics, Aachen, June 3-6, 1991, DGLR-Bericht 91-06 (1991), 91-071.

16. Schewe, G., "Beispiele für Kraft-messungen im Windkanal mit piezoelektrischen Mehrkomponenten-meßelementen", ZFW 14 (1990), pp. 32-37.